DOI 10.1007/s11018-020-01801-4
Measurement Techniques, Vol. 63, No. 5, August, 2020

MEDICAL AND BIOLOGICAL MEASUREMENTS

HIGH-PRECISION TEMPERATURE MEASUREMENT SYSTEM FOR MAGNETIC RESONANCE IMAGING

D. S. Semenov,[1] V. A. Yatseev,[2] E. S. Akhmad,[1]
Yu. A. Vasilev,[1] K. A. Sergunova,[1] and A. V. Petraikin[1]

UDC 681.78

To determine the compliance of an implantable medical device with the safety requirements in magnetic resonance imaging, an experimental assessment of the heating of this device during a study is necessary. The use of traditional methods, such as thermocouple measurements or radiation thermometry, is difficult in the conditions of a magnetic resonance imaging room. A spectrometric system for measuring temperature in conditions of a magnetic resonance imaging room is proposed. The developed system has a sensitivity of 0.01°C and an error of 0.1% in the range of 10–50°C. The temperature sensors used in the system are Fabry–Perot interferometers. The design of the sensors and the method of calibration are described. The system was tested in determining the heating of two passive implants during the study in a magnetic resonance imager with a magnetic field induction of 1.5 T. The compliance of the developed system with the recommendations adopted in magnetic resonance imaging for evaluating the heating of implantable medical devices is demonstrated. The temperature value obtained is comparable with the value found during testing of this implant according to ASTM F 2182. The presented measuring system can be used to assess the magnetic resonance compatibility of implantable medical devices, to develop scanning protocols for patients with metal structures, as well as to confirm or refine mathematical models of heat transfer.

Keywords: *magnetic resonance imaging, heating in an electromagnetic field, temperature measurement, fiber optic systems, Fabry–Perot sensor, broadband interferometry, implantable medical devices.*

Introduction. Magnetic resonance imaging (MRI) is one of the most widespread methods of medical imaging. Unlike other x-ray methods, this method does not involve patient radiation exposure. However, constant and variable electromagnetic fields lead to the emergence of certain risk factors, including thermal response of tissues. The first data on tissue heating during magnetic resonance were published in the 1980s, however, the performed experiments mainly related to localized temperature changes [1]. A significant contribution to the description of the effects of electromagnetic fields of MRI was made by Shellock [2–4]. Heating of implantable medical devices due to the occurrence of currents in them, which appear as a result of interaction with alternating magnetic fields, is an important factor to consider for ensuring safety. The International Electrotechnical Commission (IEC) has developed MRI safety requirements currently in force in Russia as GOST MEK 60601-2-33, "Medical Electrical Equipment. Part 2-33. Particular Safety Requirements Taking into Account the Basic Functional Characteristics of Medical Diagnostic Equipment Operating on the Basis of Magnetic Resonance," and limiting the maximum local heating of body tissues during the study. American College of Radiology (ACR), in turn, proposed

[1] Research and Practical Clinical Center for Diagnostics and Telemedicine Technologies, Moscow Health Care Department, Moscow, Russia; e-mail: d.semenov@npcmr.ru.
[2] Kotelnikov Institute of Radio Engineering and Electronics, Russian Academy of Sciences, Moscow, Russia; e-mail: yatseev@gmail.com.

Translated from Izmeritel'naya Tekhnika, No. 5, pp. 66–71, May, 2020. Original article submitted October 25, 2019. Accepted November 25, 2019.

an experimental technique for evaluating implant heating in MRI, described in ASTM F 2182 [5]. This technique is actively used in practice to confirm theoretical studies [6]. In addition, the test result is taken into account when determining the type of magnetic resonance compatibility of the implant: safe, unsafe or compatible under certain conditions [7]. A separate task of this study is the measurement of temperature under MRI conditions, which include:

– exposure to a constant magnetic field with induction of 1.5–3.0 T and sometimes 7.0 T;

– the influence of variable gradient and radio-frequency fields acting on a gel phantom that mimics the electrophysical properties of bodily tissues [5].

The range of recorded values imposes a limitation on the accuracy of the measuring system, since a temperature change of 1°C is considered acceptable for a 6 min study in accordance with GOST MEK 60601-2-33. For some ferromagnetic objects, the heating rate does not exceed 0.05°C/min [8], and when the antenna effect occurs, heating can reach 60°C [9].

The purpose of this work is to solve the problem of high-precision measurement of heating of implantable medical devices in an MRI room. The use of thermocouple measurements or radiation thermometry is impossible due to sensitivity to electrical noise, lack of data on emissivity, the influence of extraneous radiation, etc. Therefore, it seems optimal to use optical systems in which the readings of a thermosensitive element are read out by a light beam that is not exposed to external influences. At the same time, the light beam has a number of characteristic features, such as wavelength, direction of propagation, etc., which makes it possible to distinguish it relative to the background signal and interference.

Justification for the development of the system. The following fiber-optic sensors are mainly used for temperature measurement: fluorimetric [10, 11], one based on fiber Bragg gratings [12, 13] and a Fabry–Perot interferometer [6, 14–16]. The most common fiber-optic temperature and strain gauges are sensors based on Bragg gratings [12, 13, 17]. For such measurements with the help of ultraviolet laser radiation, periodic microstructures are created in the fiber [18, 19], which reflect light at a certain wavelength, depending on the lattice period and the refractive index of the fiber. When the external temperature changes, the Bragg grating parameters change, which leads to a spectral shift of the maximum of the grating reflection peak. Along with the advantages of such sensors, the main ones being a wide range of measurements and the possibility of multiplexing, i.e., placing a plurality of sensors in series on one fiber, a significant drawback is the demand for the quality of the spectrometer, which is part of the receiving unit – interrogator. As a rule, the temperature resolution of such sensors does not exceed 0.1–0.5°C, depending on the interrogation system used.

The most sensitive sensors are sensors based on interferometers, in particular, the Fabry–Perot interferometer, the principle of which was used in this work. Currently, there are several manufacturers of medical sensors on the Fabry–Perot interferometer: FISO Technologies (Canada), Opsens (Canada), RJC Enterprises (USA), etc. In the industrial production of sensors, they use fiber etching processes to form microstructures in it, such as cavities or diaphragms. This approach allows for the implementation of industrial production on the scale of several tens of thousands of units per year. The sensors have small dimensions (0.2 μm), comparable with the diameter of the fiber itself, which is an advantage for the use of these sensors when introduced into the body of a living organism [14]. As in the case of sensors based on Bragg gratings, this method of manufacturing sensors limits the sensitivity of the method used.

Sensor design. The sensor developed by the authors of this article is shown in Fig. 1 and represents the following construction: two segments of the optical fiber *1* are enclosed in a sensitive capillary *3* and are firmly affixed to it by spot welding *5*. The interferometer is formed by perpendicular chips of the fiber segments. As the temperature increases, the glass capillary and the fibers inside it elongate, but since the coefficient of expansion of glass is much higher than the coefficient of expansion of quartz fiber, the ends of the fibers begin to diverge to the sides. Compared to sensors based on Bragg gratings, the temperature measurement is not due to the thermal expansion of the quartz fiber, but depends on the expansion of the glass capillary, which has a thermal expansion coefficient that is an order of magnitude higher than that for fused silica. Therefore, sensitivity to temperature also increases by an order of magnitude. The sensitivity gain, in comparison with the sensors based on Bragg gratings, can be approximately estimated by the formula

$$K = (\alpha_g/\alpha_q)(L_{Br}/L_{F-P}),$$

where α_g, α_q temperature expansion coefficients of glass and quartz, respectively; L_{Br} is the length of the Bragg grating; L_{F-P} is the length of the Fabry–Perot sensor.

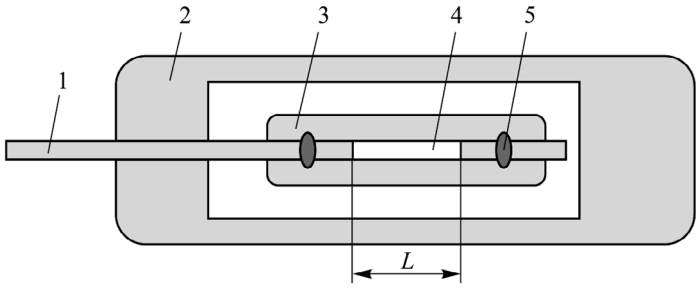

Fig. 1. Structural diagram of the sensor: *1*) optical fiber; *2*) protective capillary; *3*) sensitive capillary; *4*) optical clearance; *5*) welding points.

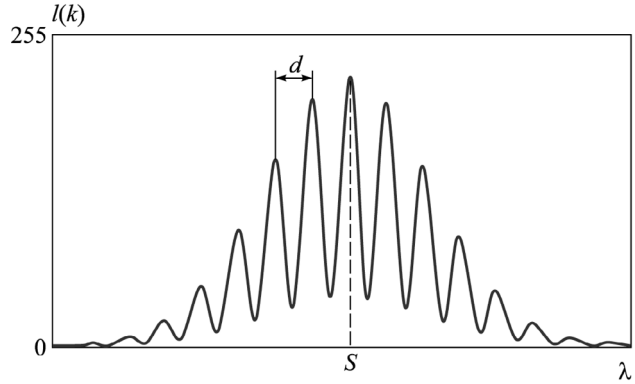

Fig. 2. Spectrum of radiation reflected from a Fabry–Perot interferometer.

With a typical Bragg grating length of several millimeters and a Fabry–Perot sensor length of ten millimeters or more, sensitivity can be increased tens or hundreds of times.

The manufacture of the sensor. One of the problems that was solved by the authors in the manufacture of sensors is the method of affixing the fiber inside the capillary. Since the range of movement of the fiber relative to the capillary during temperature measurements is from several nanometers to several micrometers, the attachment of the fiber in the capillary should provide appropriate accuracy. Various adhesives were tested, including those based on cyanides, polyurethanes, epoxies, etc. However, they could not provide long-term drift-free attachment of surfaces under the influence of temperatures of the working range 10–50°C. Therefore, the authors used the method of fiber fusion into a glass capillary using spot arc welding. The welding temperature exceeded 1000°C and was selected so as not to damage the fiber during melting and to ensure reliable attachment of the glass capillary and silica fiber. In this case, before welding, the ends of the fibers were affixed in the capillary at a distance of 50 μm. To protect against mechanical deformations, an additional glass capillary *2* sealed on one side was used (see Fig. 1). The design obtained as a result of development has sufficient strength, which is necessary when placing the sensor in a viscous gel phantom.

The principle of operation of the temperature measurement system. The measuring system consists of a twelve-channel optical measuring unit with a diffraction grating spectrometer. The specified optical unit is connected to an interrogator of optical temperature sensors. The sensors are Fabry–Perot interferometers formed by flat ends of optical fibers located at a distance L of the order of ten micrometers (see Fig. 1).

The measurement method is based on the principle of broadband interferometry, according to which a so-called white light source is used: in this case, LEDs with a spectrum width of 40 nm, the radiation from which is sent to the sensors. The radiation is reflected back from the sensors, while its spectrum undergoes changes depending on the distance between the cleaved fibers – the base of the interferometer. Further, the radiation reflected from the sensors is sent to the interrogator, in which the spectrometer decomposes the light along the wavelengths and transmits the radiation spectrum to the light-receiving matrix. An example of a sensor spectrum is shown in Fig. 2, where d is the distance between the peaks, and S is the wavelength corresponding to the largest peak in the interference pattern.

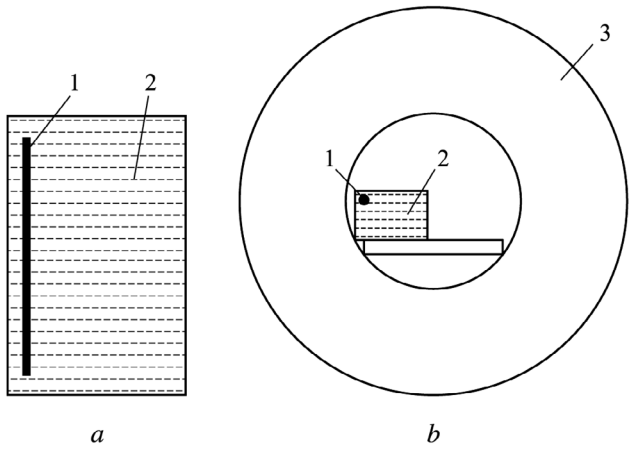

Fig. 3. Phantom (*a*) and its placement (*b*) in the tomograph: *1*) implant; *2*) gel phantom; *3*) superconducting magnet.

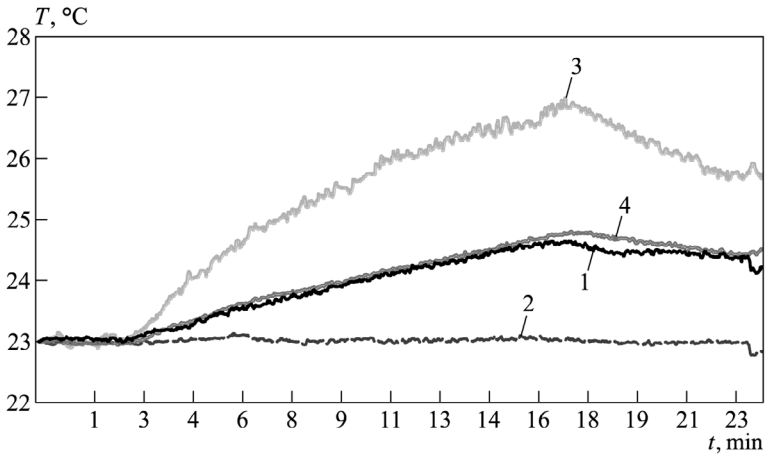

Fig. 4. Dependence of the measured temperature T on time t (time from the start of the study) for various sensors in the process of magnetic resonance research: *1*) end of the femoral shaft; *2*) head of the femoral implant; *3*) the first end of the orthopedic implant; *4*) the second end of the orthopedic implant.

To increase the sensitivity of the measurement method, a two-stage signal analysis scheme was used: at the first stage, the distance between the peaks of the interference pattern in the spectrum was analyzed and the preliminary value of L was calculated, then the positions of the peaks in the spectrum were estimated, from which the indicated value can be determined with higher accuracy. This method makes it possible to increase the sensitivity of the method for determining the distance between reflective surfaces to an accuracy of several nanometers and measure the temperature with sensitivity up to hundredths of a degree, providing the ability to measure absolute values.

Calibration of the developed system. The main physical quantity that a sensor can measure on a Fabry–Perot interferometer is the distance L between the reflecting surfaces, in this case, the cleaved fibers. To obtain the temperature as the output signal, it is necessary to carry out a calibration, i.e., to establish the dependence of the temperature on the distances between the fiber cleavage sites. Since the response of the system is linear, it is sufficient to calibrate for normalization at two values of the operating range: at the upper and lower boundaries. Calibration is ensured by placing the sensors in a liquid oil thermostat with a built-in reference temperature sensor with an accuracy of 0.05°C or higher.

Testing the measuring system. The system was tested in determining the heating of two passive implants during magnetic resonance imaging. The experimental design is shown in Fig. 3. The rectangular phantom *2*, in accordance with the recommendations of [5], was filled with hydroxyethyl cellulose gel. The position of the phantom and implant *1* relative to the isocenter of the tomograph *3* was chosen in accordance with the map of specific absorption coefficient (SAR) so as to ensure

maximum heating. The position of the implant relative to the phantom is shown in Fig. 3*a*. Temperature sensors were affixed on the surface of the implants using amagnetic tape: for the implant of the femoral joint – on the head and the end of the femoral shaft, and for an elongated orthopedic implant – at its two ends. The control unit of the measuring system was located in the technical office of the MRI room outside the Faraday cage.

The study was carried out on a Hitachi Oval 1.5T tomograph using the pulse sequence Turbo Spin Echo, *TR* = 260 ms, *TE* = 6 ms, Echo Train Length = 16, Bandwidth = 69 kHz, Flip Angle = 90°, SAR = 1.5 W/kg, the scan duration was 15 min.

For temperature control, the implants and phantom were placed in the treatment room several hours before the start of the study. Based on experimental data analysis results, the temperature measurement values were obtained that are shown in Fig. 4. In addition, as a result of the experiment, the amplitudes of heating the surface of the orthopedic implant, which amounted to 4°C in 15 min, and the implant of the hip joint – 2.5°C for 15 min, were determined. In the latter case, the data coincided with the value provided by the manufacturer.

Conclusion. A high-precision fiber-optic temperature measuring system with a sensitivity of 0.01°C was developed, compatible with the conditions of the magnetic resonance medium and the accepted methods for determining the maximum heating of implantable medical devices. The system was tested, which showed its full compliance with the requirements and made it possible to obtain values equivalent to the estimates of the manufacturer of one of the implants. The presented measuring complex can be used not only for the experimental determination of the heating of metal structures in MRI, but also for the identification, confirmation or refinement of mathematical models of heat transfer, as well as in the development of methods for the safe conduct of magnetic resonance studies for patients with implants and for demonstration purposes.

REFERENCES

1. J. A. Elder and D. F. Cahill, *Biological Effects of Radiofrequency Radiation*, Health Effects Research Laboratory, Office of Research and Development, U. S. Environmental Protection Agency, Research Triangle Park N. C. (1984).
2. F. G. Shellock, D. J. Schaefer, and C. J. Gordon, *Magn. Reson. Med.*, **3**, No. 4, 644–647 (1986).
3. F. G. Shellock, *Magn. Reson. Quart.*, **5**, No. 4, 243–261 (1989).
4. F. G. Shellock, *J. Magn. Reson. Im.*, **12**, No. 1, 30–36 (2000), DOI: 10.1002/1522-2586(200007)12:1<30: aid-jmri4> 3.0.co;2-s.
5. ASTM F2182-11a, *Standard Test Method for Measurement of Radio Frequency Induced Heating On or Near Passive Implants during Magnetic Resonance Imaging*, https://www.astm.org/Standards/F2182.htm, acc. 04.24.2018.
6. D. X. Feng, J. P. McCauley, F. K. Morgan-Curtis, et al., *Brit. J. Radiol.*, **88**, No. 1056, 20150633 (2015), DOI: 10. 1259/bjr.20150633.
7. K. A. Sergunova, E. S. Akhmad, A. V. Petryaykin, et al., "Safety of conducting magnetic resonance imaging for patients with implantable medical devices," *Byull. NTsSSKh im. Bakuleva RAMN*, **20**, No. 4, 313–323 (2019), DOI: 10.24022/1810-0694-2019-20-4-313-323.
8. Yu. A. Vasiliev, D. S. Semenov, V. A. Yatseev, et al., "An experimental study of the heating of ferromagnetic objects during magnetic resonance imaging," *Nauch.-Tekhn. Vest. Inform. Tekhnol., Mekh. Optiki*, **19**, No. 1, 173–179 (2019), DOI: 10.17586/2226-1494-2019-19-1-173-179.
9. L. P. Panych and B. Madore, *J. Magn. Reson. Im.*, **47**, No. 1, 28–43 (2018), DOI: 10.1002/jmri.25761.
10. C. Armenean, E. Perrin, M. Armenean, et al., *Magn. Reson. Med.*, No. 52, 1200–1206 (2004), DOI: 10.1002/mrm. 20246.
11. E. Neufeld, S. Kühn, G. Szekely, and N. Kuster, *Phys. Med. Biol.*, **54**, No. 13, 4151–4169 (2009), DOI: 10.1088/0031-9155/54/13/012.
12. O. V. Butov, E. M. Dianov, and K. M. Golant, *Meas. Sci. Technol.*, **17**, 975–979 (2006), DOI: 10.1088/0957-0233/ 17/5/S06.
13. M. Ramakrishnan, G. Rajan, Y. Semenova, and G. Farrell, *Sensors*, **16**, No. 1, 99–126 (2016), DOI: 10.3390/ s16010099.

14. V. A. Korolev and V. T. Potapov, “Biomedical fiber optic temperature and pressure sensors,” *Med. Tekhn.*, **272**, No. 2, 38–42 (2012).
15. A. N. Sokolov and V. A. Yatseev, “Fiber-optic sensors and systems: principles of construction, capabilities and prospects,” *LightWave Russ.*, No. 4, 44–46 (2006).
16. A. M. Zotov, P. V. Korolenko, and V. A. Yatseev, “Algorithms for fast signal processing of a fiber-optic Fabry–Perot interferometer,” *Datch. Sistemy*, No. 4, 29–33 (2018).
17. O. V. Butov, A. P. Bazakutsa, Y. K. Chamorovskiy, et al., *Sensors*, **19**, No. 19, 4228 (2019), DOI: 10.3390/s19194228.17.
18. O. V. Butov, *Results Phys.*, **15**, 102542 (2019), DOI: 10.1016/j.rinp.2019.102542.
19. S. A. Vasiliev, O. I. Medvedkov, and I. G. Korolev, “Fiber gratings of the refractive index and their application,” *Kvant. Elektron.*, **35**, No. 12, 1085–1103 (2005), DOI: 10.1070/QE2005v035n12ABEH013041.